2013

Polypyrrole doped with redox-active poly(2-methoxyaniline-5-sulfonic acid) for lithium secondary batteries

Yang Yang
University of Wollongong, yy922@uowmail.edu.au

Caiyun Wang
University of Wollongong, caiyun@uow.edu.au

Syed A. Ashraf
University of Wollongong, syed@uow.edu.au

Gordon G. Wallace
University of Wollongong, gwallace@uow.edu.au

Publication Details

Yang, Y., Wang, C., Ashraf, S. & Wallace, G. G. (2013). Polypyrrole doped with redox-active poly(2-methoxyaniline-5-sulfonic acid) for lithium secondary batteries. RSC Advances, 3 (16), 5447-5452.

Polypyrrole doped with redox-active poly(2-methoxyaniline-5-sulfonic acid) for lithium secondary batteries

Abstract
Polypyrrole is a promising electrode material for flexible/bendable energy storage devices due to its inherent fast redox switching, mechanical flexibility, easy processability and being environmentally benign. However, its low attainable capacity limits its practical applications. Here, we synthesise a polypyrrole/poly(2-methoxyaniline-5-sulfonic acid) (PPy/PMAS) composite by incorporating redox-active PMAS into a PPy matrix via an electropolymerization method. For comparison, polypyrrole containing the electrochemically inert dopant p-toluenesulfonate (PPy-pTS) was prepared under the same conditions. The resultant PPy/PMAS film shows greatly improved electrochemical properties by harnessing the contribution from PMAS, i.e. higher specific capacity, better rate capability and improved cycling stability when used as a cathode material in a lithium secondary battery. It delivers a high specific capacity of 120.6 mAh g-1 at a current density of 0.1 A g-1, and retains about 88.5% of the capacity (106.7 mAh g-1) over 800 consecutive cycles at a high current density of 1 A g-1.

Keywords
sulfonic, 5, methoxyaniline, 2, batteries, poly, secondary, active, redox, doped, polypyrrole, lithium, acid

Disciplines
Engineering | Physical Sciences and Mathematics

Publication Details
Yang, Y., Wang, C., Ashraf, S. & Wallace, G. G. (2013). Polypyrrole doped with redox-active poly(2-methoxyaniline-5-sulfonic acid) for lithium secondary batteries. RSC Advances, 3 (16), 5447-5452.

Polypyrrole Doped with Redox-Active Poly(2-methoxyaniline-5-sulfonic acid) for Lithium Secondary Batteries

Yang Yang, Caiyun Wang*, Syed Ashraf and Gordon G.Wallace*

Polypyrrole is a promising electrode material in flexible/bendable energy storage devices due to its inherent fast redox switching, mechanical flexibility, easy processability and being environmentally benign. However, its low attainable capacity limits its practical applications. Here, we synthesise polypyrrole/poly(2-methoxyaniline-5-sulfonic acid) (PPy/PMAS) composite by incorporating redox-active PMAS into a PPy matrix via an electropolymerization method. For comparison, polypyrrole containing the electrochemically inert dopant *p*-toluenesulfonate anion (PPy-*p*TS) is prepared under the same conditions. The resultant PPy/PMAS film shows greatly improved electrochemical properties by harnessing the contribution from PMAS, i.e. higher specific capacity, better rate capability and cycling stability when used as a cathode material in a lithium secondary battery. It delivers a high specific capacity of 120.6 mAh g^{-1} at a current density of 0.1 A g^{-1}, and retains about 88.5% of the capacity (106.7 mAh g^{-1}) over 800 consecutive cycles at a high current density of 1 A g^{-1}.

Introduction

Recently, strong interest has been aroused in flexible or bendable energy storage devices such as rollup displays and wearable electronic devices.[1-3] In the pursuit of a new generation of flexible/bendable storage devices, inherently conducting polymers (ICPs) have attracted research interest due to their inherent fast redox switching, high conductivity, mechanical flexibility, lightweight, easy processability, and being environmentally benign.[4-7] However, their low attainable specific capacity has limited their practical application in battery technologies, because of the dead weight from the electrochemically inert counter-ion dopants. Take the well-known polypyrrole (PPy)/*p*-toluenesulfonate *(p*TS) (0.33 doping level) as an example, its theoretical specific capacity is 133 mAh g^{-1} if only taking the pyrrole units weight into account. It turns out to be only 73 mA g^{-1} when the weight of dopant is also included.

A strategy to overcome this problem is to dope redox-active anions into the ICP matrix.[8-10] The electroactive dopants can contribute to the quantity of charge that can be stored, thus leading to higher specific capacity. Using the electroactive dopant anthraquinone-1-sulfonate, PPy films exhibited a high energy density of 150 Ah L^{-1}, which was more than twice that observed for PPy films containing electrochemically inactive anions such as naphthalene-1-sulfonate or ClO_4^-.[11] Iron-redox-couple, $Fe(CN)_6^{4-}$, doped PPy was synthesized by chemical polymerization of pyrrole monomer using ammonium persulfate oxidant in an aqueous $Na_4Fe(CN)_6$ solution.[12] This electrode delivered an enhanced redox capacity of 140 mAh g^{-1} at a constant current density of 50 mA g^{-1}. Recently, polypyrrole doped with biopolymers lignosulfonate (PPy/Lig), was electropolymerized. It clearly demonstrated that the electrochemical activity of this composite derived from both PPy and lignin-derived quinines, and the charge density and capacitance delivered were comparable to polypyrrole combined with nanostructured carbons.[13]

Poly(2-methoxyaniline-5-sulfonic acid) (PMAS), one type of conductive and electroactive polymer,[14] can be incorporated into polypyrrole or polyaniline matrix as a dopant. The resultant polymers have shown attractive properties for a wide range of applications.[15-17] Liu et al. reported that PPy/PMAS films exhibited lower impedance and were better substrates for L929 cell adhesion and proliferation than PPy/NO_3 films.[16] PPy/PMAS composites also exhibited improved cathodic expansion, which is promising for soft actuators application.[18,19] Moreover, polyaniline (PANI)/PMAS coated carbon fibre increased the capacitance from 125 to as high as 222 F g^{-1} (69% improvement), due to the capacitive behaviour of the PANI/PMAS composite.[20]

In this work using PMAS as a dopant, a PPy/PMAS composite was prepared via an electropolymerization method from aqueous solution. The incorporation of redox-active PMAS is expected to enhance its available charge storage. Also this large polyelectrolyte anion, might affect the polypyrrole growth and its properties. A common type of polypyrrole, polypyrrole containing the dopant *p*-toluenesulfonate anion (PPy-*p*TS), was also synthesized under the same conditions for comparison. Their electrochemical properties were investigated as a cathode material in lithium batteries. The as-synthesized PPy/PMAS film demonstrated greatly improved electrochemical properties, a much higher capacity of 120.6 mAh g^{-1} at the discharge current density of 100 mA g^{-1} and excellent cycling stability with about 88.5% of capacity retention over 800 consecutive cycles at a high current density of 1 A g^{-1}.

Experimental

Materials synthesis

PMAS was synthesized chemically by the polymerization of 5 g (0.025 mol) 2-Methoxy aniline-5-sulfonic acid (MAS) dissolved in 50 mL of water (milli-Q) at pH 4 as adjusted by adding NH_3 (28% w/w). To this stirred solution 7.14 g (0.031 mol) of ammonium persulfate oxidant dissolved in 25 mL of water was added and stirred overnight to complete the reaction. The temperature was kept between 5-10 °C during the whole process. PMAS was purified by a cross flow dialysis system. GPC results show Mn 3200; Mw 22000; PDI 5.

PPy/*p*TS or PPy/PMAS film was galvanostatically electrodeposited on a stainless steel mesh (Hongye Stainless Steel Wire Cloth Co. Ltd.) from an aqueous solution containing the dopant and 0.1 M pyrrole monomer. The concentration of sodium *p*-toluenesulfonate and PMAS used in this work was 1 mg mL^{-1}, respectively. The applied current density was 1 mA cm^{-2} and the amount of charge consumed was 0.6 C cm^{-2}.

Characterization

Thermogravimetric analysis (TGA) was performed in nitrogen flow (90 ml min^{-1}) at a heating rate of 10 ºC min^{-1}, using a TA Instruments' Q500 Thermogravimetric Analyzer. The samples were dried in a vacuum oven at 60 ºC overnight before TGA test. The surface morphologies of the films were investigated using a field emission SEM (FESEM, JEOL JSM7500FA). The conductivity measurement of the films was performed using a four-probe technique (RM3, JANDEL). UV-visible (UV-vis) spectra were recorded using a UV spectrophotometer (UV-1800, Shimadzu) in the range from 270 nm to 1100 nm. A thin layer of PPy/*p*TS or PPy/PMAS composite film was electrodeposited on indium tin oxide (ITO) coated glass at a current density of 0.5 mA cm^{-1} for 2 minutes for the UV-vis measurements.

Electrochemical measurements

PPy/*p*TS and PPy/PMAS films were dried in a vacuum oven at 60 ºC overnight, and the electrodes were assembled into LR 2032 type coin cells coupled with lithium foil in a glove box. The electrolyte used was 1.0 M $LiPF_6$ in 1:1 (v/v) ethylene carbonate (EC): dimethylcarbonate (DMC). Cyclic voltammetry (CV) of the cell was performed using a Solartron SI 1287 and scanned between 2 V to 4.0 V at a scan rate of 5 mV s^{-1}. Electrochemical impedance spectra (EIS) measurements were performed using a Gamry EIS 3000™ system, and the frequency range spanned from 100 kHz to 0.1 Hz with an AC amplitude of 10 mV at open circuit potential. The EIS results were analyzed by using Zview software. Galvanostatic charge/discharge and cycling tests were performed using a battery test system (Land CT2001A, Wuhan Jinnuo Electronics Co. Ltd.). The specific capacities of the samples were calculated based on the mass of the PPy/*p*TS or the PPy/PMAS active material, and the average weight of each sample was approximately 0.5 mg. All the batteries were subjected to an activation process, 20 charge/discharge cycles at a current density of 100 mA g^{-1} prior to data recording, except for the EIS measurements for as-fabricated cells.

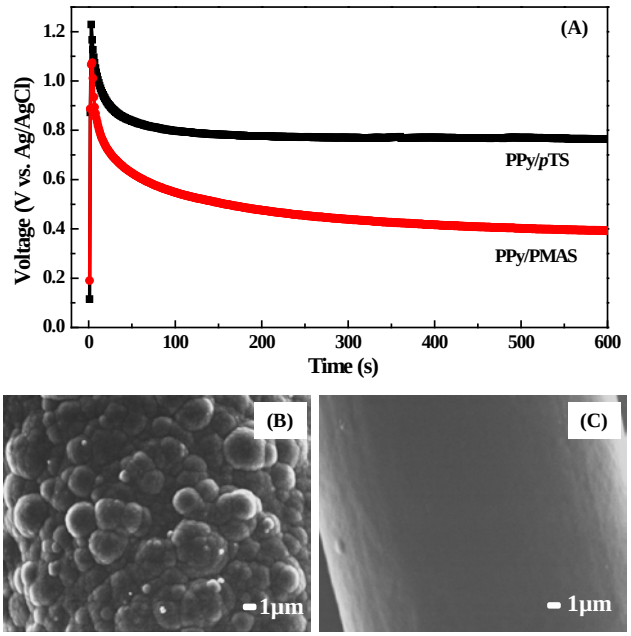

Figure 1. Chronopotentiograms for PPy/*p*TS and PPy/PMAS growth (A); FESEM images of surface morphology of PPy/*p*TS film (B) and PPy/PMAS film (C) on stainless steel mesh.

Result and Discussion

Using conditions described in the Experimental Section it was found that they all formed a coherent, adherent film on the working electrode with either *p*TS or PMAS as dopant. Their chronopotentiograms (Figure 1A) all exhibited an initial spike due to higher potential needed for oxidation of monomer, followed by a slow potential decrease as polymer growth proceeded and approached a steady potential of ca. 0.76 V and 0.4 V for PPy/*p*TS and PPy/PMAS, respectively. This enhanced polymer growth for PPy/PMAS, suggested from its much lower deposition potential, can be attributed to the unique dual function of PMAS as dopant. The presence of PMAS effectively facilitates the chain propagation due to supramolecular pre-ordering of PMAS template effect. In addition, charge transfer during the polymerization is also enhanced, not just through the polypyrrole network but also via the PMAS chain since PMAS itself is a conducting polymer.[21] PPy/*p*TS exhibited a typical cauliflower morphology composed of large nodules (Figure 1B), while a very smooth surface was observed for the PPy/PMAS (Figure 1C) due to the supramolecular pre-ordering template effect of PMAS.

The elemental analysis (%) results for the PPy/PMAS composite are: C 48.44, N 11.6, S 6.32 and H 3.83. The ratio between pyrrole unit and 2-methoxyaniline-5-sulfonic acid (MAS) unit is 3.2, deduced from the obtained N/S ratio. It means that approximately three pyrrole units are doped with one MAS unit. Based on the well-acknowledged PPy and PMAS structures,[22] the structures of PPy/PMAS is proposed and illustrated in scheme 1. Given that one electron transfer is contributed from every three pyrrole units and another one electron is available from every MAS unit, the theoretical capacity of this composite is 130.5 mAh g^{-1}.

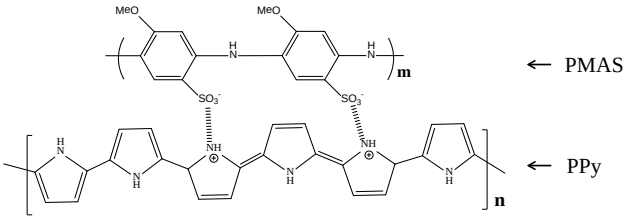

Scheme 1 Chemical structures of polypyrrole and Poly (2-methoxyaniline-5-sulfonic acid)

The thermal stability of PPy/*p*TS, PPy/PMAS composites and pure PMAS are depicted in Figure 2 (A). A sharp mass transition occurring at about 200 ºC is attributed to degradation of PMAS and loss of SO_3H groups in the polymer chains as reported for pure PMAS.[23, 24] The mass loss of PMAS over the temperature range between 200 to 300 ºC was 30.8 %, compared to only 4.5 % mass loss found for PPy/*p*TS. The difference of the mass loss results from the lower decomposition temperature of the PMAS.[23, 24] A mass loss of 12.2 % was obtained for PPy/PMAS composite over the same temperature range. It was much higher than that for PPy/ *p*TS, which can be ascribed to the presence of PMAS in the polypyrrole matrix.

As-synthesized PPy/*p*TS film shows an absorption peak at 475 nm and free carrier tail beyond 600 nm, characteristics of polypyrrole (Figure 2 (B)). This absorption peak is related to the electron transition from valence band to antibipolaron band, and the tail is due to electron transition from the valence band to the bipolaron band.[25] An additional sharp peak centered at 359 nm was observed for PPy/PMAS composite film, which is assigned to π–π* transition observed for PMAS.[14, 21] These results clearly demonstrate the successful incorporation of PMAS into

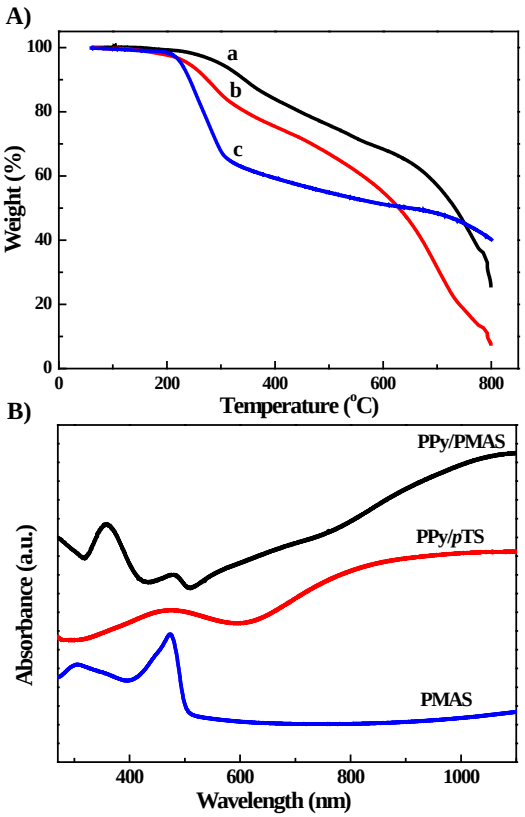

Figure 2. (A) TGA curves of PPy/*p*TS film (a), PPy/PMAS film (b) and pure PMAS film (c); (B) UV-Vis spectra of PPy/*p*TS and PPy/PMAS films on ITO glass.

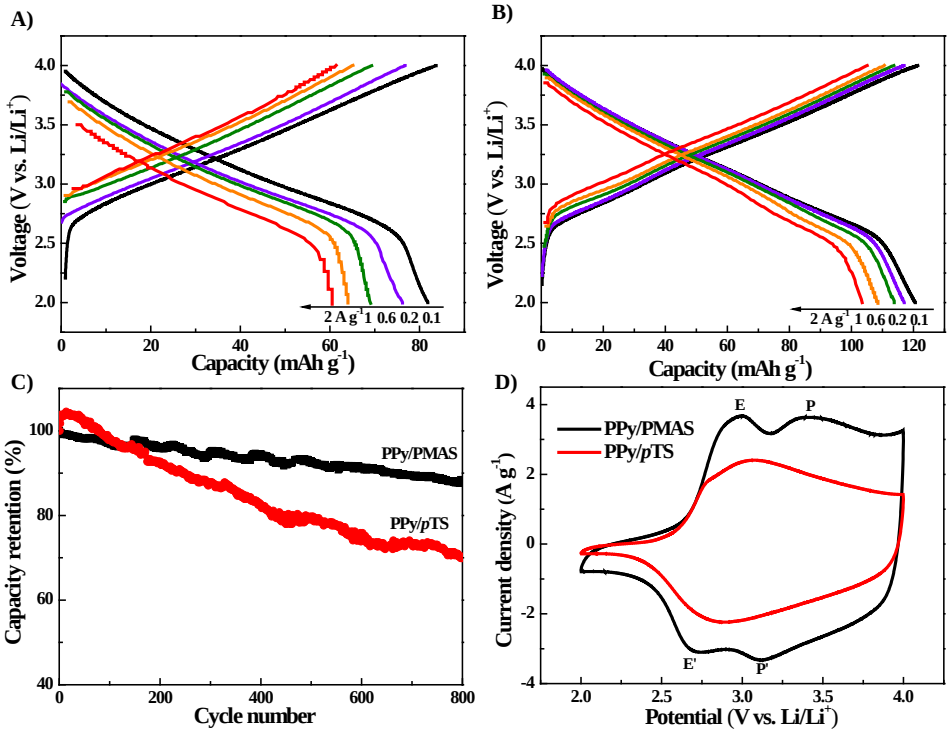

Figure 3. Electrochemical data for PPy/ *p*TS and PPy/PMAS composite films on stainless steel mesh substrate in lithium-ion batteries in the potential window of 2.0 - 4.0 V (vs Li/Li^+). (A) Voltage profiles for PPy/*p*TS film at different current rate. (B) Voltage profiles for PPy/PMAS film at different current rate. (C) Capacity retention versus cycle number at 1 A g^{-1} for PPy/*p*TS and PPy/PMAS films. (D) Cyclic voltammograms of PPy/*p*TS and PPy/PMAS composites films at a scan rate of 5 mV s^{-1}.

polypyrrole.

The charge/discharge curves of either PPy/PMAS or the PPy/*p*TS film in a lithium secondary battery are shown in Figure 3A and 3B. A specific capacity of 81 mAh g^{-1} was obtained for PPy/*p*TS at a current density of 0.1 A g^{-1}, close to the highest capacity of 85 mAh g^{-1} reported recently for PPy/*p*TS.[26] A much higher specific capacity of 120.6 mAh g^{-1} was obtained for the PPy/PMAS electrode at the same current density, about 40 mAh g^{-1} more than that of PPy/*p*TS. Such great capacity enhancement could be ascribed to the contribution from the redox-active PMAS dopant. This capacity (120.6 mAh g^{-1}) is close to its theoretical capacity, suggesting this composite we obtained had good electrochemical properties.

PPy/PMAS delivered a specific capacity of 117, 113, 108 and 103 mAh g^{-1} at the current densities of 0.2, 0.6, 1 and 2 A g^{-1} respectively. It exhibited an excellent rate capability with a capacity retention of 85.7 % at 2 A g^{-1} with respect to that obtained at 0.1 A g^{-1}. In comparison, PPy/*p*TS delivered a specific capacity of 76.2, 69, 64 and 60.5 mAh g^{-1} at the current densities of 0.2, 0.6, 1 and 2 A g^{-1} respectively. About 74% of the capacity was retained at 2 A g^{-1} compared with those obtained at 0.1 A g^{-1}. The better rate capability of PPy/PMAS could be attributed to its unique electrically conducting network created by template effect of PMAS, which facilitates the movement of ion and electron (as shown in the Figure 1).

PPy/PMAS composites electrode also exhibited a greatly improved cycling stability compared with PPy/*p*TS at a high current density of 1 A g^{-1} (Figure 3c). About 88.5% of the initial capacity was retained over 800 consecutive cycles, in contrast to 67.1% capacity retention for PPy/*p*TS. For polypyrrole-type battery electrodes, their charge/discharge processes are associated with concomitant expulsion/insertion of anions or the insertion/expulsion of cations as shown in Equations (1) and (2),

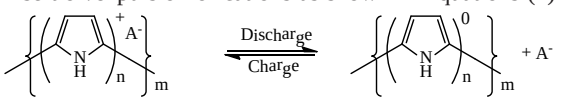

... (1)

and/or

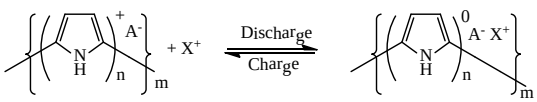

... (2)

respectively.[27] The insertion/expulsion of cations is the dominant processes for polypyrrole with large/less immobile dopants.[28,29] The capacity deterioration for PPy/*p*TS over cycling can be explained by the swelling and shrinking of the polypyrrole film.[30, 31] With less mobile or immobile polyelectrolyte PMAS as dopant in the PPy/PMAS composite, the movement of the much smaller size cations predominates the charge/discharge processes, thus limiting the swelling and shrinking of polypyrrole film and leading to the improved cycling stability.

The cyclic voltammograms obtained using either PPy/*p*TS or PPy/PMAS composites as the working electrode are shown in Figure 3d. PPy/*p*TS displayed a pair of broad redox peaks at the electrochemical window of 2.0-4.0 V (vs Li/Li^+), typical for polypyrrole-type electrode in lithium secondary batteries.[32] Two pairs of cathodic/anodic peaks (E/E' and P/P') with cathodic peaks at about 2.7 and 3.1 V (vs Li/Li^+) were observed for PPy/PMAS electrode, characteristics of polyaniline-based conducting polymers. The redox pair (E/E') is attributed to the interconversion between the leucoemeraldine and emeraldine states of PMAS, and another redox couple (P/P') results from the interconversion of the emeraldine to the pernigraniline state of PMAS.[33, 34] It clearly demonstrates that PMAS has been successfully incorporated into the polymer matrix, further supporting the conclusion from UV-vis results. It is also noticed that the broad redox peaks from PPy was not distinguishable. They were covered by the sharp PMAS redox peaks. PPy/PMAS generated much higher current response than PPy/*p*TS within the applied potential window, suggesting that the incorporation of redox-active PMAS dopant enhanced the electrochemical properties of polypyrrole. This conclusion is in agreement with that obtained from the charge/discharge results.

AC impedance spectroscopy is an electrochemical tool used to

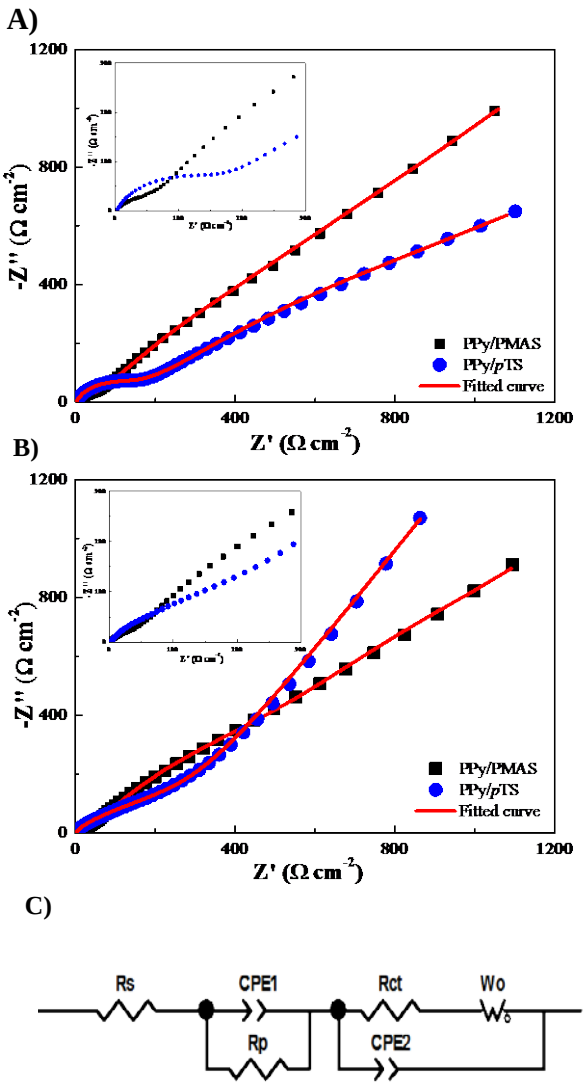

Figure 4. Experimental (symbol) and simulated (line) Nyquist plots for PPy/*p*TS and PPy/PMAS composite films on stainless steel mesh in lithium secondary battery. (A) as-fabricated PPy/*p*TS and PPy/PMAS composite films; (B) after 800 consecutive charge/discharge cycles at a current density of 1 A g^{-1}; (C) The equivalent circuit used for the simulation.

Table 1. Electrode resistance obtained from the Nyquist analysis using the equivalent circuit.

Electrode	Rs (Ω cm^{-2})	Rp (Ω cm^{-2})	Rct (Ω cm^{-2})
PPy/*p*TS (as-fabricated)	2.8	150	58.8
PPy/PMAS (as-fabricated)	2.4	132.4	31.2
PPy/*p*TS (after cycling)	3.2	285.6	174.8
PPy/PMAS (after cycling)	2.4	192	41.2

characterize or detect the kinetic limitations in the system under investigation. The Nyquist plots of PPy/*p*TS and PPy/PMAS electrodes, at the as-fabricated state or after 800 consecutive charge/discharge cycles, were investigated. Generally, they all exhibited a depressed semicircle in the high frequency and an inclined line close to 45^{o} in the low frequency (Figure 4A and 4B). To get a deeper insight, these plots were simulated using the equivalent circuit as shown in Figure 4C.[35,36] In the circuit, Rs is the bulk resistance of the electrolyte; Rp and Rct is ion transfer resistance and charge transfer resistance, respectively. The constant phase elements, CPE1 and CPE2, are associated with double-layer capacities across the substrate/PPy and PPy/electrolyte solution interfaces, respectively; Wo corresponds to Warburg impedance resulting from the semi-infinite diffusion of ions in the electrode at the low frequency. The fitting results, including Rs, Rp and Rct are summarized in Table 1.

The as-fabricated PPy/PMAS electrode exhibited a lower Rp and Rct compared with those of PPy/*p*TS electrode, 150 vs. 132.4 Ω cm^{-2} and 58.8 vs. 31.2 Ω cm^{-2}, respectively. It might be ascribed to the unique structure of PPy/PMAS, which provides a convenient pathway for charge transfer and ion transfer and effectively reduces the resistance. Rp and Rct increased after 800 consecutive charge/discharge cycles at a current density of 1 A g^{-1} for both PPy/*p*TS and PPy/PMAS. The increase of the cell resistance is responsible for the capacity fade as shown in Figure 3C. PPy/PMAS demonstrated an Rp increase of 45% and Rct increase of 32%, respectively. A much higher resistance increase was shown for PPy/*p*TS, with 90% Rp increase and 197% Rct increase after the cycling. This can be used to explain the poorer cycling stability delivered by PPy/*p*TS.

Conclusions

In summary, we have demonstrated that the incorporation of redox-active PMAS dopant into the polypyrrole matrix greatly improved its electrochemical properties when used as a cathode material in lithium secondary batteries. PPy/PMAS composite film delivered almost 50% more specific capacity at a current density of 0.1 A g^{-1} than PPy/*p*TS film. The contribution from PMAS can be evidenced from the cyclic voltammograms. PPy/PMAS composite film also exhibited an enhanced cycling stability, about 88.5% capacity retention (vs. 67.1% for PPy/pTS) over 800 consecutive cycles at a high current density of 1 A g^{-1}. The lesser increase in electrode resistance for PPy/PMAS is responsible for its improved cycling stability. This can be explained by the limited swelling and shrinkage of PPy/PMAS film due to the predominant small size cations movement during the charge/discharge processes, leading to the improved cycling stability as the resistance increase was suppressed. The electrochemical properties could be further improved by optimizing the electrodeposition parameters or using other redox-active dopants with higher specific capacity. Using redox-active dopants for conducting polymers is an avenue to enhance their electrochemical properties.

Acknowledgements

Financial support from the Australian Research Council is gratefully acknowledged. Yang Yang acknowledges the support of the CSC Scholarship from the Ministry of Education of P.R. China. The authors gratefully acknowledge A/Prof. Chee O. Too for his proof-reading of this manuscript. The authors also acknowledge use of facilities within UOW Electron Microscopy Centre.

Notes and References

ARC Centre of Excellence for Electromaterials Science, Intelligent Polymer Research Institute, AIIM Facility, University of Wollongong, NSW 2500, Australia.

* Corresponding authors:
Dr. Caiyun Wang
Email: caiyun@uow.edu.au
Tel.: +61 2 42981426
Fax: +61 2 4298 3114.

Prof. Gordon G. Wallace
E-mail: gwallace@uow.edu.au
Tel: +61 2 42213127
Fax: +61 2 42213114

1. H. Gwon, H. S. Kim, K. U. Lee, D. H. Seo, Y. C. Park, Y. S. Lee, B. T. Ahn and K. Kang, *Energy Environ. Sci.*, 2011, **4**, 1277-1283.
2. K. T. Nam, D. W. Kim, P. J. Yoo, C. Y. Chiang, N. Meethong, P. T. Hammond, Y. M. Chiang and A. M. Belcher, *Science*, 2006, **312**, 885-888.
3. H. Nishide and K. Oyaizu, *Science*, 2008, **319**, 737-738.
4. G. A. Snook, P. Kao and A. S. Best, *J. Power Sources*, 2011, **196**, 1-12.
5. L. Nyholm, G. Nyström, A. Mihranyan and M. Strømme, *Adv. Mater.*, 2011, **23**, 3751-3769.

6. G. Nyström, A. Razaq, M. Strømme, L. Nyholm and A. Mihranyan, *Nano Lett.*, 2009, **9**, 3635-3639.
7. C. Wang, W. Zheng, Z. Yue, C. O. Too and G. G. Wallace, *Adv. Mater.*, 2011, **23**, 3580-3584.
8. K. S. Park, S. B. Schougaard and J. B. Goodenough, *Adv. Mater.*, 2007, **19**, 848-851.
9. H. K. Song and G. T. R. Palmore, *Adv. Mater.*, 2006, **18**, 1764-1768.
10. G. Torres-Gómez, E. M. Tejada-Rosales and P. Gómez-Romero, *Chem. Mater.*, 2001, **13**, 3693-3697.
11. H. Yoneyama, Y. Li and S. Kuwabata, *J. Electrochem. Soc.*, 1992, **139**, 28-32.
12. M. Zhou, J. Qian, X. Ai and H. Yang, *Adv. Mater.*, 2011, **23**, 4913-4917.
13. G. Milczarek and O. Inganäs, *Science*, 2012, **335**, 1468-1471.
14. F. Masdarolomoor, P. C. Innis, S. Ashraf and G. G. Wallace, *Synth. Met.*, 2005, **153**, 181-184.
15. F. Masdarolomoor, P. C. Innis, S. Ashraf, R. B. Kaner and G. G. Wallace, *Macromol. Rapid Commun.*, 2006, **27**, 1995-2000.
16. H. Zhao and G. G. Wallace, *Polym. Gels and Netw.*, 1998, **6**, 233-245.
17. X. Liu, K. J. Gilmore, S. E. Moulton and G. G. Wallace, *J. Neural Eng.*, 2009, **6**, 1-10.
18. W. Takashima, H. Hashimoto, K. Tominaga, A. Tanaka, S. S. Pandey and K. Kaneto, *Thin Solid Films*, 2010, **519**, 1093-1099.
19. A. Tanaka, W. Takashima and K. Kaneto, *Thin Solid Films*, 2006, **499**, 179-184.
20. G. J. Wilson, M. G. Looney and A. G. Pandolfo, *Synth. Met.*, 2010, **160**, 655-663.
21. F. Masdarolomoor, P. C. Innis and G. G. Wallace, *Electrochim. Acta*, 2008, **53**, 4146-4155.
22. G. G. Wallace, G. M. Spinks, L. A. P. Kane-Maguire and P. R. Teasdale, *Conductive Electroactive Polymers: Intelligent Polymer Systems, Third Edition*, Taylor & Francis, 2008.
23. K. S. Jang, H. Lee and B. Moon, *Synth. Met.*, 2004, **143**, 289-294.
24. G. Cakmak, Z. Küçükyavuz and S. Küçükyavuz, *Synth. Met.*, 2005, **151**, 10-18.
25. D. Y. Kim, J. Y. Lee, D. K. Moon and C. Y. Kim, *Synth. Met.*, 1995, **69**, 471-474.
26. I. Sultana, M. M. Rahman, S. Li, J. Wang, C. Wang, G. G. Wallace and H. K. Liu, *Electrochim. Acta*, 2012, **60**, 201-205.
27. A. Talaie and G. G. Wallace, *Synth. Met.*, 1994, **63**, 83-88.
28. K. Naoi, M. Lien and W. H. Smyrl, *J. Electrochem. Soc.*, 1991, **138**, 440-445.
29. C. Wang, P. G. Whitten, C. O. Too and G. G. Wallace, *Sens. Actuators B Chem.*, 2008, **129**, 605-611.
30. P. Novák, K. Müller, K. S. V. Santhanam and O. Haas, *Chem. Rev.*, 1997, **97**, 207-282.
31. T. Shimidzu, A. Ohtani, T. Iyoda and K. Honda, *J. Electroanal .Chem.*, 1987, **224**, 123-135.
32. J. G. Killian, B. M. Coffey, F. Gao, T.O. Poehler and P. C. Searson, *J. Electrochem. Soc.*, 1996, **143**, 936-942.
33. B. L. He, B. Dong, W. Wang and H. L. Li, *Mater. Chem. Phys.*, 2009, **114**, 371-375.
34. G. Yang, W. Hou, X. Feng, L. Xu, Y. Liu, G. Wang and W. Ding, *Adv. Funct. Mater.*, 2007, **17**, 401-412.
35. M. D. Levi and D. Aurbach, *J. Electrochem. Soc.*, 2002, **149**, E215-E221.
36. U. Rammelt, S. Bischoff, M. El-Dessouki, R. Schulze, W. Plieth and L. Dunsch, *J. Solid State Electr.*, 1999, **3**, 406-411.